

EXPRESS LETTER

Open Access



Recovery process of shear wave velocities of volcanic soil in central Mashiki Town after the 2016 Kumamoto earthquake revealed by intermittent measurements of microtremor

Yoshiya Hata^{1*}, Masayuki Yoshimi², Hiroyuki Goto³, Takashi Hosoya⁴, Hitoshi Morikawa⁵ and Takao Kagawa⁶

Abstract

An earthquake of JMA magnitude 6.5 (foreshock) hit Kumamoto Prefecture, Japan, at 21:26 JST on April 14, 2016. Subsequently, an earthquake of JMA magnitude 7.3 (main shock) hit Kumamoto and Oita Prefectures at 1:25 JST on April 16, 2016. The two epicenters were located adjacent to central Mashiki Town, and both events caused significantly strong motions. The heavy damage including collapse of residential houses was concentrated in “Sandwich Area” between Prefectural Route 28 and Akitsu River. During the main shock, we have successfully observed strong motions at TMP03 in Sandwich Area. Simultaneously with installation of the seismograph at TMP03 on April 15, 2016, between the foreshock and the main shock, a microtremor measurement was taken. After the main shock, intermittent measurements of microtremor at TMP03 were also taken within December 6, 2016. As the result, recovery process of shear wave velocities of volcanic soil at TMP03 before/after the main shock was revealed by time history of peak frequencies of the microtremor H/V spectra. Using results of original PS logging tests at proximity site of TMP03 on July 28, 2016, the applicability for the shear wave velocities to TMP03 was then confirmed based on similarity between the theoretical and monitored H/V spectra.

Keywords: Microtremor measurement, H/V spectrum, Shear wave velocity, Strong motion

Background

The 2016 Kumamoto earthquake as named by the Japan Meteorological Agency (JMA) is a series of earthquakes that started with the earthquake of JMA magnitude 6.5 at a shallow depth in northwest region of Kumamoto Prefecture, Kyushu Island, Japan, at 21:26 JST on April 14, 2016. Subsequently, a larger earthquake of JMA magnitude 7.3 occurred at 1:25 JST on April 16, 2016, 28.0 h after the first event. Hereafter, we call the first event on April 14 the “foreshock” and the second event on April 16 the “main shock.” Central Mashiki Town, which is located

close to the two epicenters of the foreshock and the main shock, was exposed to significantly strong motions and suffered significant damage (see Fig. 1). In the heavily damaged zone in central Mashiki Town including Sandwich Area (Hata et al. 2016a), the ratio of totally collapsed wooden houses due either to the foreshock or to the main shock exceeded 50% (e.g., Sugino et al. 2016), resulting in a significant loss of lives.

During the main shock, Hata et al. (2016b) were given an unexpected opportunity to observe strong motions at TMP01, TMP02 and TMP03 as shown in Fig. 1. The observed strong motions at TMP03 exceeded the largest observed ground motions during the 1995 Kobe earthquake in terms of spectral acceleration and JMA seismic intensity (Nishimae 2004) and have a significant importance to the engineering as well as seismological

*Correspondence: hata@civil.eng.osaka-u.ac.jp

¹ Graduate School of Engineering, Osaka University, 2-1 Yamada-oka, Suita, Japan

Full list of author information is available at the end of the article

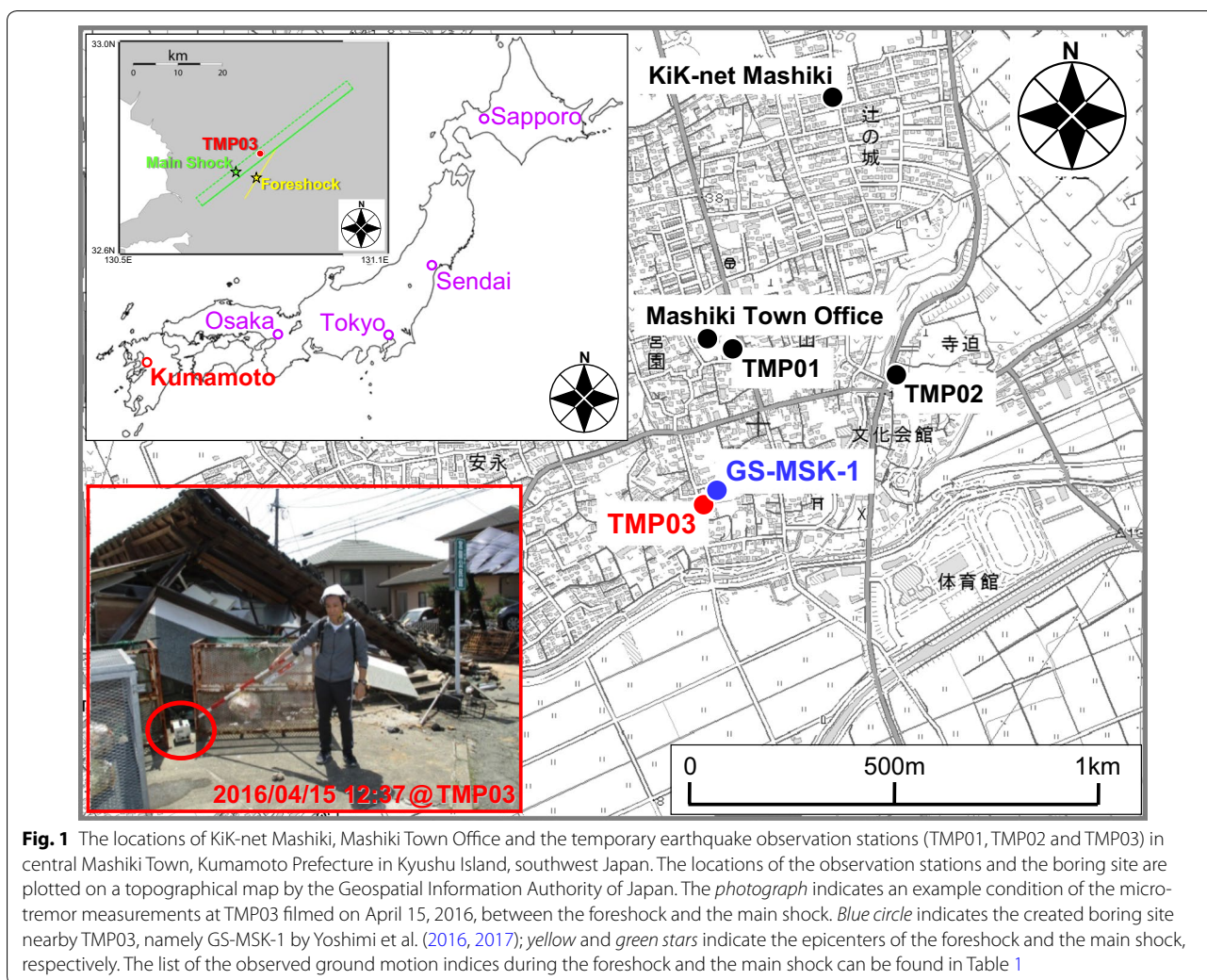


Fig. 1 The locations of KiK-net Mashiki, Mashiki Town Office and the temporary earthquake observation stations (TMP01, TMP02 and TMP03) in central Mashiki Town, Kumamoto Prefecture in Kyushu Island, southwest Japan. The locations of the observation stations and the boring site are plotted on a topographical map by the Geospatial Information Authority of Japan. The *photograph* indicates an example condition of the microtremor measurements at TMP03 filmed on April 15, 2016, between the foreshock and the main shock. *Blue circle* indicates the created boring site nearby TMP03, namely GS-MSK-1 by Yoshimi et al. (2016, 2017); *yellow and green stars* indicate the epicenters of the foreshock and the main shock, respectively. The list of the observed ground motion indices during the foreshock and the main shock can be found in Table 1

communities (Hata et al. 2016a). With installation of the seismograph at TMP03 on April 15, 2016, between the foreshock and the main shock, Hata et al. (2016c) have previously conducted microtremor measurement in order to confirm the validity as a candidate site for the temporary earthquake observation (see photograph in Fig. 1). After the main shock, intermittent measurements of microtremor at TMP03 were also carried out within December 6, 2016, in order to evaluate recovery process of properties of subsurface soil for this study.

Previous studies have reported a phenomenon in which shear modulus of soil is decreased during a large earthquake and then gradually recovers over a time interval of several months (e.g., Arai 2006; Houlsby and Wroth 1991; Nagao et al. 2016; Nishimura et al. 2005; Sugito et al. 2000; Rubinstein et al. 2007; Tokimatsu and Hosaka 1986; Vlastos et al. 2006). It is important to fully understand such a

phenomenon, because it could be related to the dissipation of excess pore water pressure and hence to a potential long-term deformation of soil after a large earthquake. However, in spite of its importance, there have been relatively few field data with respect to the recovery process of shear modulus of soil after a large earthquake.

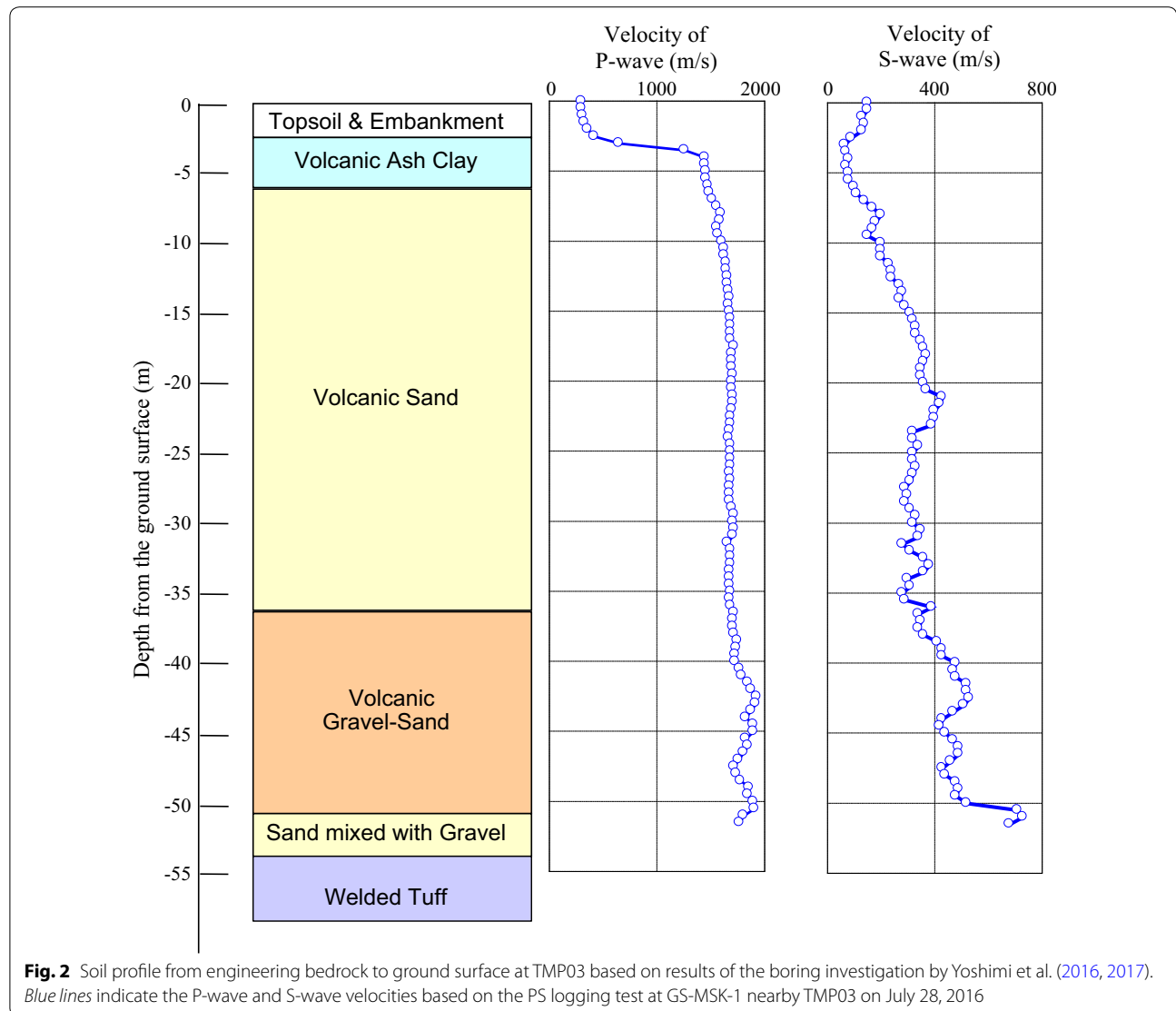
Since we confirmed the similar phenomenon at TMP03 based on the intermittent measurements of microtremor, the obtained results were reported in this express letter. In particular, the recovery process based on the time history of peak frequencies of the microtremor H/V spectra at TMP03 after the main shock was confirmed. We also confirmed the similarity between the monitored H/V spectrum at TMP03 and the theoretical ones based on original PS logging tests at proximity site of TMP03 (Yoshimi et al. 2016, 2017), indicating applicability for the observed shear wave velocities to TMP03.

Methods

The microtremor measurement was intermittently conducted at TMP03 (see Fig. 1) after the foreshock including just after the main shock. At GS-MSK-1 nearby TMP03 (see Fig. 1), a PS logging test was performed on July 28, 2016, by Yoshimi et al. (2016, 2017) and revealed depth distribution for the P-wave and S-wave velocities with 50-cm interval to engineering bedrock as shown in center and right panels of Fig. 2. In left panel of Fig. 2, we also obtained the subsurface consisting mainly of volcanic soil. Figure 1 shows the observed JMA seismic intensities during the foreshock and the main shock at the earthquake observation stations including TMP03. In Fig. 1, the largest JMA seismic intensity (6.9) in central Mashiki Town during the main shock was observed at TMP03 (Hata et al. 2016a, b). The initial measurement

of microtremor at TMP03 was conducted 15.2 h after the foreshock, that is, 12.8 h before the main shock (Hata et al. 2016c). After the main shock, the earliest measurement was taken 32.0 h after the foreshock, that is, 4.0 h after the main shock. Then, the measurement was taken intermittently 5657 h after the foreshock (i.e., 5629 h after the main shock).

In particular, the measurements were taken 15.2, 32.0, 43.6, 67.5, 206, 449, 494, 710, 831, 902, 1219, 2513, 3062, 3640, 4280, 4933 and 5657 h after the foreshock. The measurement was also taken for three components (NS, EW and UD). The arithmetic mean of the two horizontal components was adopted in the calculation of the H/V spectral ratio. The measurement was taken for one hour (≈ 163.84 s \times 22 sections), and the sampling frequency was 100 Hz. The specifications of the instrument for



the microtremor measurement were the same as those reported in Senna et al. (2006).

The comparison of the microtremor H/V spectra at TMP03 is shown in Fig. 3. The procedure to calculate the H/V spectra can be summarized as follows: First, a high-pass filter of 0.1 Hz was adopted, and seven time sections of 163.84 s each were extracted from the original data considering recorded noise. Next, Fourier amplitude spectra for these seven time sections were calculated with a Parzen window of a band width of 0.05 Hz. Then, a microtremor H/V spectral ratio was calculated for each of the seven time sections, where the mean of the horizontal two components was adopted as the numerator. Finally, the spectral ratio was averaged for the seven time sections. Here, the frequency range to evaluate the microtremor H/V spectral ratio was from 0.2 to 10 Hz considering the performance of the instrument for the microtremor measurements (Senna et al. 2006). More details about the procedure to calculate the H/V spectra can be found in Hata et al. (2014b).

Monitored microtremor H/V spectra

Figure 3 clearly shows the time dependence of the peak frequencies of the calculated microtremor H/V spectra. In Fig. 3a, features of the H/V spectra such as the peak frequency and the spectral shape between 15.2 and 5657 h after the foreshock (i.e., between 12.8 h before the main shock and 5629 h after the main shock) have a good agreement. This agreement suggests that the ground motion due to the foreshock did not cause obvious changes of the microtremor H/V spectrum. As a current stage, we imagine following two explanations for the obscure changes. The estimated ground motions at TMP03 during the foreshock were smaller than the observed ones during the main shock based on the differences of the observation records at KiK-net Mashiki and Mashiki Town Office between the foreshock and the main shock (see Table 1). Moreover, although the significant changes just after the foreshock had occurred, the rough changes were recovered 15.2 h after the foreshock which we measured microtremor at TMP03. As a future study, we will perform a numerical analysis simulation in order to explain our two imaginations.

On the other hand, the peak frequency just after the main shock (see Fig. 3b) was significantly lower than the final peak frequency 5657 h after the foreshock (i.e., 5629 h after the main shock), indicating the reduction of the shear wave velocities of the volcanic soil. Note, at KiK-net Mashiki (see Fig. 1), we have already confirmed that the same significant change of H/V spectral ratio featuring spectral shape and peak frequency has not occurred just before/after the main shock. Then the peak frequency gradually increased and approached to

the final value (nearly equal to the initial value), indicating the recovery process of the shear wave velocities. The H/V spectrum about 2500 h after the foreshock and the main shock was almost identical to that before the main shock (see Fig. 3l). Thus, the recovery process of the shear wave velocities of the volcanic soil at TMP03 was clearly documented in the monitored microtremor H/V spectra.

Recovery process of shear wave velocities

Figure 4 plots the time dependence of the peak frequencies of the monitored microtremor H/V spectra at TMP03 15.2, 32.0, 43.6, 67.5, 206, 449, 494, 710, 831, 902, 1219, 2513, 3062, 3640, 4280 and 4933 h after the foreshock divided by that 5657 h after the foreshock. Here, although the averaged H/V spectral ratios for different measured time are calculated from seven time sections of 163.84 s extracted from the observed microtremor data, we have confirmed that same value of the peak frequencies is shown in the all seven time sections. In Fig. 4, the ratios gradually increased after the main shock and reached almost 1.0 in about 1000 h after the foreshock (nearly equal to after the main shock). The final peak frequency 5657 h after the foreshock (i.e., 5629 h after the main shock) has recovered to that 15.2 h after the foreshock (i.e., 12.8 h before the main shock). Thus, we can find the recovery process of shear wave velocities of volcanic soil in central Mashiki Town after the main shock of the 2016 Kumamoto earthquake, the end time for the process, and can conjecture that the end time for the process is almost 5629 h after the main shock. On the other hand, the beginning time for the process was not estimated due to the effects of much large-scale aftershocks just after the main shock.

Figure 3l also shows the comparison of the theoretical with monitored H/V spectral ratios at TMP03. In Fig. 3l, the monitored H/V spectral ratio was based on the measurement results of microtremor at TMP03 during the PS logging test at GS-MSK-1 on July 28, 2016. On the other hand, the theoretical H/V spectral ratio (e.g., Haskell 1953) based on the fundamental mode Rayleigh wave was calculated from the soil profiles at GS-MSK-1 nearby TMP03 (see Fig. 2) with the conventional soil densities (Goto et al. 2017). We can find a good agreement between the monitored and theoretical H/V spectral ratios as shown in Fig. 3l, indicating applicability for detection of the shear wave velocities of the volcanic soil at TMP03 with good accuracy by the monitoring results.

Summary and conclusions

In this study, the recovery process of shear wave velocities of subsurface soil after the 2016 Kumamoto earthquake sequence at a heavily damage site in central Mashiki Town, Japan, was revealed by intermittent measurements

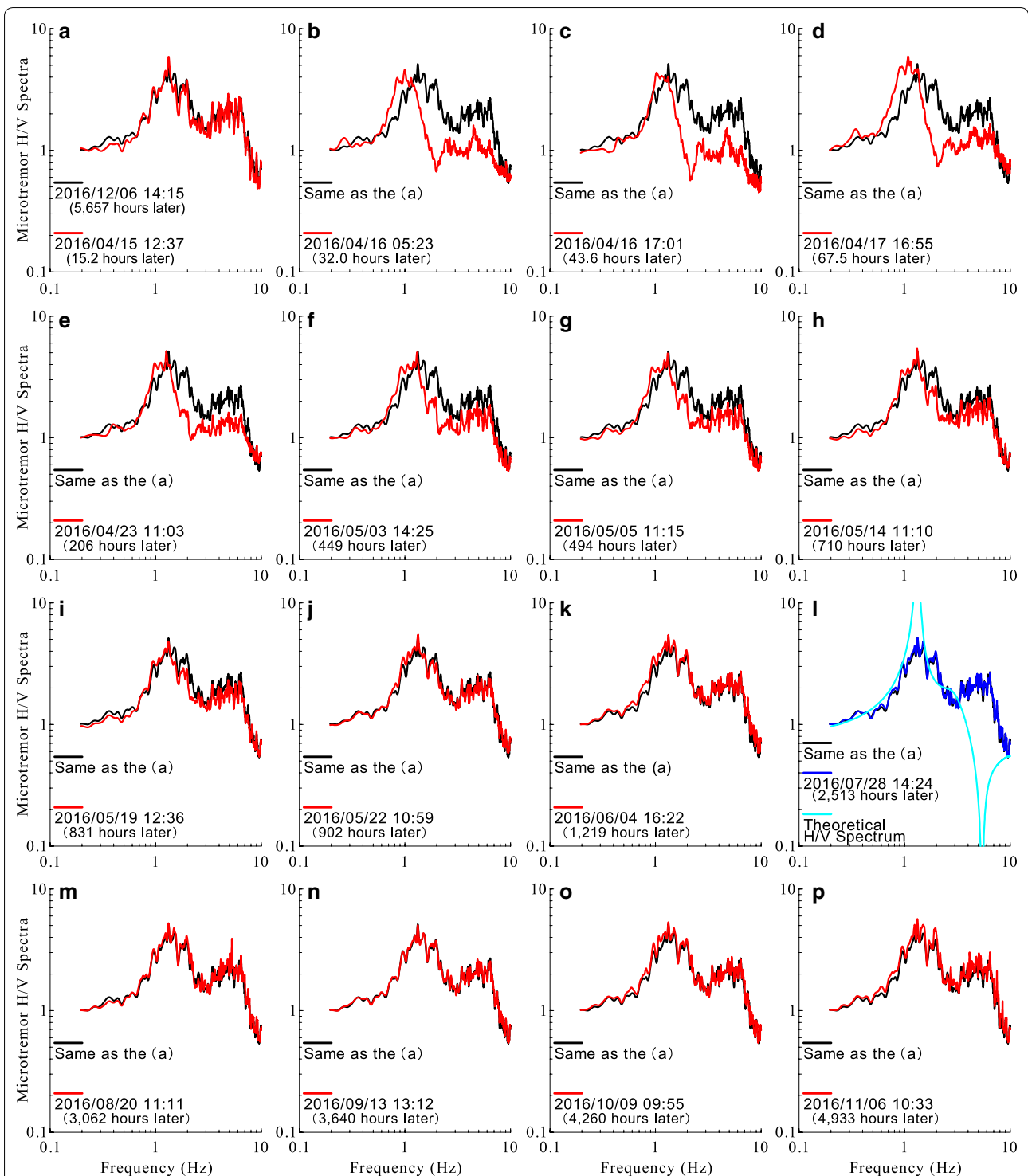


Fig. 3 Comparison of the monitored microtremor H/V spectral ratios after the foreshock at TMP03. *Black lines* (see **a–k** and **m–p**) indicate the H/V spectral ratios measured on December 6, 2016; *red lines* (see **a–k** and **m–p**) indicate the spectra measured on April 15, April 16, April 17, April 23, May 3, May 5, May 14, May 19, May 22, June 4, August 20, September 13, October 9 and November 6, 2016, respectively; *blue line* (see **l**) indicates the spectrum measured on July 28, 2016, during the PS logging tests by Yoshimi et al. (2016; 2017); *light blue line* (see **l**) indicates the theoretical H/V spectral ratio based on the results of the PS logging tests at GS-MSK-1 nearby TMP03 (see center and right panels in Fig. 2)

Table 1 List of the observed ground motion indices at permanent and temporary stations in central Mashiki Town during the 2016 Kumamoto earthquake sequence (e.g., Hata et al. 2016b)

	KiK-net Mashiki	Mashiki Town Office	TMP01	TMP02	TMP03
Foreshock					
PGAs (m/s ²) [N-S]	7.59	6.32	-	-	-
PGAs (m/s ²) [E-W]	9.23	7.32	-	-	-
PGAs (m/s ²) [U-D]	14.0	33.8	-	-	-
PGVs (m/s) [N-S]	0.77	1.18	-	-	-
PGVs (m/s) [E-W]	0.91	1.36	-	-	-
PGVs (m/s) [U-D]	0.55	0.15	-	-	-
JMA seismic intensities	6.4	6.6	-	-	-
Main shock					
PGAs (m/s ²) [N-S]	6.53	7.72	9.02	7.37	9.18
PGAs (m/s ²) [E-W]	11.6	8.26	14.9	11.5	11.6
PGAs (m/s ²) [U-D]	8.73	6.68	10.0	9.76	7.02
PGVs (m/s) [N-S]	0.85	0.97	1.06	1.05	1.33
PGVs (m/s) [E-W]	1.32	1.77	1.59	1.64	1.79
PGVs (m/s) [U-D]	0.47	0.51	1.06	0.63	0.72
JMA seismic intensities	6.5	6.7	6.6	6.7	6.9

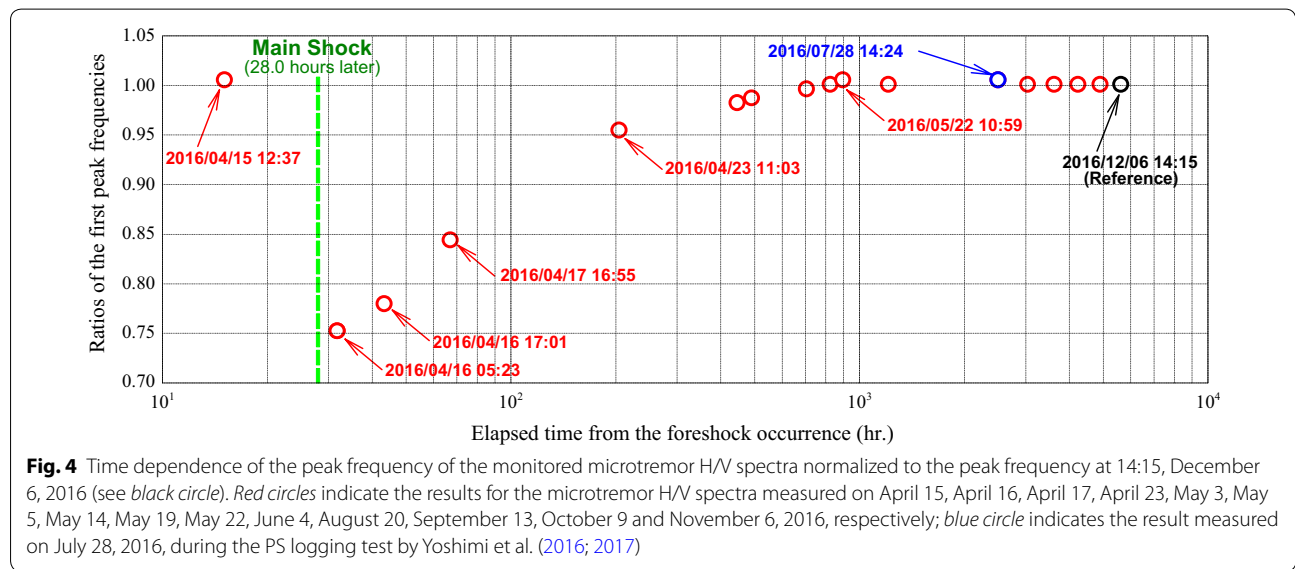


Fig. 4 Time dependence of the peak frequency of the monitored microtremor H/V spectra normalized to the peak frequency at 14:15, December 6, 2016 (see black circle). Red circles indicate the results for the microtremor H/V spectra measured on April 15, April 16, April 17, April 23, May 3, May 5, May 14, May 19, May 22, June 4, August 20, September 13, October 9 and November 6, 2016, respectively; blue circle indicates the result measured on July 28, 2016, during the PS logging test by Yoshimi et al. (2016; 2017)

of microtremor for about 5600 h before/after the main shock. The results of the study can be summarized as follows:

1. The recovery process of shear wave velocities of the volcanic soil was clearly documented in the time-dependent peak frequency of the measured microtremor H/V spectra.
2. The measured microtremor H/V spectrum at the site of interest during the PS logging test after the main shock nearby the site of interest was repro-

duced good accurately in the theoretical H/V spectrum based on the fundamental mode Rayleigh wave, which indicates that the P-wave and S-wave velocities distribution after the main shock was detectable with good accuracy by the monitoring results.

As a future study, we would like to simulate the obtained recovery process of the shear wave velocities based on dynamic FEM analyses considering pore water pressure with observed strong motions for the main shock and major large aftershocks.

Authors' contributions

YH conducted the measurement and the simulation. YH, MY and HG drafted the manuscript. MY and TH acquired data of the ground investigation. HG, HM and TK participated in reconnaissance survey of the seismic damage around TMP03. MY, HG, HM and TK participated in the discussion and the interpretation. All authors read and approved the final manuscript.

Author details

¹ Graduate School of Engineering, Osaka University, 2-1 Yamada-oka, Suita, Japan. ² Geological Survey of Japan, National Institute of Advanced Industrial Science and Technology, 1-1-1 Higashi, Tsukuba, Japan. ³ Disaster Prevention Research Institute, Kyoto University, Gokasho, Uji, Japan. ⁴ Solution Center, Chuo Kaihatsu Corporation, 3-13-5 Nishi-waseda, Shinjuku Ward, Tokyo, Japan. ⁵ School of Environment and Society, Tokyo Institute of Technology, 4259, Nagatsuta, Midori Ward, Yokohama, Japan. ⁶ Graduate School of Engineering, Tottori University, 4-101 Minami, Koyama, Tottori, Japan.

Acknowledgements

The authors thank the residents of Mashiki Town and a staff of Mashiki Town Office for generously cooperating in conducting the microtremor measurements. The authors also appreciate the assistance of Mr. Fumihito Minato, a graduate student of Osaka University, during the measurement. This study was partially supported by JSPS KAKENHI (Grant No. JP15H05532), and the special research fund for collaborative research in Disaster Prevention Research Institute (DPRI), Kyoto University (Grant Number: 28U-05 and 28U-07). This study was carried out as an activity of the Subcommittee on Aggregation and Application of Seismic Trace Data in Geographical Feature [Head: Prof. Kazuo Konagai (Yokohama National University)], the Subcommittee on Mechanism of Earthquake Motion around Active Fault [Head: Prof. Takao Kagawa (Tottori University)] and the Subcommittee on Survey Analysis of Damage for the 2016 Kumamoto Earthquake Sequence [Head: Prof. Takaaki Ikeda (Nagaoka University of Technology)], organized by the Earthquake Engineering Committee, Japan Society of Civil Engineers [Chairperson: Prof. Sumio Sawada (DPRI, Kyoto University)].

Competing interests

The authors declare that they have no competing interests.

Data and resources

Strong motion data at TMP01, TMP02 and TMP03 can be obtained from Division of Dynamics of Foundation Structures, Disaster Prevention Research Institute (DPRI), Kyoto University, at <http://www.wcatfish.dpri.kyoto-u.ac.jp/~kumaq/> (last accessed February 2017).

Publisher's Note

Springer Nature remains neutral with regard to jurisdictional claims in published maps and institutional affiliations.

Received: 19 February 2017 Accepted: 16 May 2017

Published online: 22 May 2017

References

- Arai H (2006) Detection of subsurface Vs recovery process using microtremor and weak ground motion records in Ojiya, Japan. In: Proceedings of 3rd international conference on urban earthquake engineering, Tokyo, Japan, pp 631–638. <https://www.researchgate.net/publication/228444135>
- Goto H, Hata Y, Yoshimi M (2017) Relationship between heavily damage area due to the 2016 Kumamoto earthquakes and seismic response characteristics in central Mashiki Town, vol 87, no 2. KAGAKU, Iwanami Shoten Publishers, pp 186–191. <https://www.iwanami.co.jp/book/b280147.html>. (in Japanese)
- Haskell NA (1953) The dispersion of surface waves on multilayered media. Bull Seismol Soc Am 43(1):17–34. <http://www.bssaonline.org/content/43/1/17.abstract>
- Hata Y, Nozu A, Ichii K (2014b) Variation of earthquake ground motions within very small distance. Soil Dyn Earthq Eng 66:429–442. doi:10.1016/j.soildyn.2014.08.006
- Hata Y, Goto H, Yoshimi M (2016a) Characteristics of the observed strong ground motions in the serious damage area, Mashiki Town during the main shock of the 2016 Kumamoto Earthquake, vol 86, no 9. KAGAKU, Iwanami Shoten Publishers, pp 934–941. <http://www.iwanami.co.jp/book/b273801.html>. (in Japanese)
- Hata Y, Goto H, Yoshimi M (2016b) Preliminary analysis of strong ground motions in the heavily damaged zone in Mashiki Town, Kumamoto, Japan, during the main shock of the 2016 Kumamoto Earthquake ($M_w7.0$) observed by a dense seismic array. Seismol Res Lett 87(5):1044–1049. doi:10.1785/0220160107
- Hata Y, Goto H, Yoshimi M, Furukawa A, Morikawa H, Ikeda T, Kagawa T (2016c) Preliminary report of ground motion estimation in Mashiki Town centre for the 2016 Kumamoto earthquake sequence based on ground investigations with very high density. In: Proceedings of the 44th symposium of earthquake ground motion (2016)—what happened during the 2016 Kumamoto earthquake? AIJ, Tokyo, pp 35–46. <http://news-sv.aij.or.jp/kouzou/s4/>. (in Japanese with English abstract)
- Houlsby GT, Wroth CP (1991) The variation of shear modulus of a clay with pressure and over-consolidation ratio. Soils Found 31(3):138–143. doi:10.3208/sandf1972.31.3_138
- Nagao T, Lohani TN, Fukushima Y, Ito Y, Hokugo A, Oshige J (2016) A study on the correlation between ground vibration characteristic and damage level of structures at Mashiki Town by the 2016 Kumamoto Earthquake. In: Proceedings of 36th national conference on JSCE earthquake engineering, Kanazawa, Japan. Paper No. 913. <http://committees.jsce.or.jp/eec2/node/77>. (in Japanese with English abstract)
- Nishimae Y (2004) Observation of seismic intensity and strong ground motion by Japan Meteorological Agency and local governments in Japan. J Jpn Assoc Earthq Eng 4(3):75–78. doi:10.5610/jaee.4.3_75
- Nishimura T, Tanaka S, Yamawaki T, Yamamoto H, Sano T, Sato M, Nakahara H, Uchida N, Hori S, Sato H (2005) Temporal changes in seismic velocity of the crust around Iwate volcano, Japan, as inferred from analyses of repeated active seismic experiment data from 1998 to 2003. Earth Planets Space 57:491–505. doi:10.1186/BF03352583
- Rubinstein JL, Uchida N, Beroza GC (2007) Seismic velocity reductions caused by the 2003 Tokachi-Oki Earthquake. J Geophys Res Solid Earth. doi:10.1029/2006JB004440
- Senna S, Adachi S, Ando H, Araki T, Iisawa K, Fujiwara H (2006) Development of microtremor survey observation system. In: Proceedings of Japan geoscience union meeting, Makuahri, Japan, pp 14–18. <http://ci.nii.ac.jp/naid/10018357183>. (in Japanese)
- Sugito M, Oka F, Yashima A, Furumoto Y, Yamada K (2000) Time-dependent ground motion amplification characteristics at reclaimed land after the 1995 Hyogoken Nambu Earthquake. Dev Geotech Eng 84:145–158. doi:10.1016/S0165-1250(00)80013-9
- Sugino M, Yamamuro R, Kobayashi S, Murase S, Ohmura S, Hayashi Y (2016) Analyses of building damages in Mashiki Town in the 2016 Kumamoto Earthquake. J Jpn Assoc Earthq Eng 16(10):69–85. doi:10.5610/jaee.16.10_69
- Tokimatsu K, Hosaka Y (1986) Effects of sample disturbance on dynamic properties of sand. Soils Found 26(1):53–64. doi:10.3208/sandf1972.26.53
- Vlastos S, Liu E, Main IG, Schoenberg M, Narteau C, Li XY, Maillol B (2006) Dual simulations of fluid flow and seismic wave propagation in a fractured network: effects of pore pressure on seismic signature. Geophys J Int 166(2):825–838. doi:10.1111/j.1365-246X.2006.03060.x
- Yoshimi M, Hata Y, Goto H, Hosoya T, Morita S, Tokumaru T (2016) Borehole exploration in heavily damaged area of the 2016 Kumamoto Earthquake, Mashiki Town, Kumamoto. In: Proceedings of annual fall meeting 2016 of the Japanese society for active fault studies, Tokyo, Japan, Paper No. 17. http://jsaf.info/pdf/meeting/2016/2016fall_S.pdf. (in Japanese)
- Yoshimi M, Goto H, Hata Y, Yoshida N (2017) Nonlinear site response at the worst-hit area of the 2016 Kumamoto earthquakes in the Mashiki Town, Japan. In: Proceedings of annual meeting 2017 of Disaster Prevention Research Institute, Kyoto University, Uji, Japan, Paper No. A05. http://www.dpri.kyoto-u.ac.jp/web_j/hapyo/17/pdf/A05.pdf. (in Japanese with English abstract)